Multiscale Model. Simul.
Vol. 0, No. 0, pp. 000–000

INTERACTION BETWEEN SWITCHING DIFFUSIVITIES AND CELLULAR MICROSTRUCTURE*

PATRICK MURPHY†, PAUL C. BRESSLOFF†, AND SEAN D. LAWLEY†

Abstract. Single-particle tracking experiments have recently found that *C. elegans* zygotes rely on space-dependent switching diffusivities to form intracellular gradients during cell polarization. The relevant proteins switch between fast-diffusing and slow-diffusing states on timescales that are much shorter than the timescale of diffusion or gradient formation. This manifests in models as a small parameter, allowing an asymptotic analysis of the gradient formation. In this paper we consider how this mechanism of rapidly switching diffusive states interacts with a locally varying periodic microstructure in the cell, incorporated through a second small parameter. We show that an asymptotic analysis based on both small parameters yields different results based on the order of limits taken and suggest an explicit relation between the two parameters for when each type of analysis is appropriate. We further investigate a mean first passage time problem for a diffusing protein to gain insight into the effects of the microstructure on the global environment.

Key words. cell polarization, switching diffusivities, cellular microstructure, homogenization, multiple scales

AMS subject classifications. 92C37, 35B27

DOI. 10.1137/19M1271245

1. Introduction.

There has been a recent growth of interest in heterogeneous diffusion within biological cells [1], driven by advances in single-particle tracking (SPT) experiments, which track the trajectories of individual macromolecules within the plasma membrane by attaching an observable tag such as a quantum dot, gold nanoparticle, or a fluorophore [12, 8, 9]. These experiments have demonstrated that, rather than moving freely, molecules tend to exhibit heterogenous dynamics, including confined and anomalous diffusion. The most common method for analyzing SPT data is to detect deviations from free diffusion based on the mean squared displacement (MSD). That is, the MSD of unconfined Brownian motion is a linear function of time, whereas a sublinear temporal variation of MSD is indicative of movement in a confined environment, and a supralinear variation suggests directed motion. However, one limitation of MSD as a measure of heterogeneous diffusion is that it is based on the statistics of multiple trajectories. A more effective statistical method is to use parametric models of heterogeneous diffusion, based on the hidden Markov model (HMM) framework [5, 10, 13]. These latter studies suggest that particles within the plasma membrane can switch between different discrete conformational states with different diffusivities. Such switching could be due to interactions between proteins and the actin cytoskeleton [5] or due to protein-lipid interactions [15].

Motivated by the above experimental studies, we previously analyzed a model of a Brownian particle that randomly switches between two distinct conformational states with different diffusivities [2, 3]. We assumed that in each state the particle undergoes normal diffusion (additive white noise) but took the switching rates to de-

*Received by the editors June 28, 2019; accepted for publication February 12, 2020; published electronically DATE.
https://doi.org/10.1137/19M1271245
Funding: The second author was supported by the National Science Foundation (DMS-1613048 and IOS-1755431).
†Department of Mathematics, University of Utah, Salt Lake City, UT 84112 (pmurphy@math.utah.edu, bressloff@math.utah.edu, lawley@math.utah.edu).

pend on spatial position. We showed that in the fast switching limit $\epsilon \to 0$, where ϵ is some dimensionless scale factor, one obtains Brownian motion with a space-dependent diffusivity of the Itô form; see also [6, 7]. We also extended the theory to include colored additive noise with correlation time κ. We found that the nature of the effective multiplicative noise process obtained by taking both the white-noise limit ($\kappa \to 0$) and fast switching limit ($\epsilon \to 0$) depends on the order the two limits are taken. More specifically, taking the white-noise limit $\kappa \to 0$ first yields an Itô stochastic differential equation (SDE), whereas a Stratonovich SDE is obtained when the fast switching limit $\epsilon \to 0$ is taken first. Moreover, the form of the effective diffusion coefficient differs in the two cases. (The latter result holds even in the case of space-independent transition rates, where one obtains additive noise processes with different diffusion coefficients.)

Independently of our theoretical work, an experimental and computational study has found that *C. elegans* zygotes rely on space-dependent switching diffusivities as a mechanism for the formation of intracellular gradient formation during cell polarization [14]. During asymmetric cell division a pair of RNA-binding proteins muscle excess-5 (MEX-5) and pharynx and intestine in excess-1 (PIE-1) form opposing subcellular concentration gradients in the absence of a local source due to a spatially heterogeneous switching process. That is, both proteins switch between fast-diffusing and slow-diffusing states on timescales that are much shorter (seconds) than the timescale of gradient formation (minutes). Moreover, the switching rates are strongly polarized along the anterior/posterior axis of the zygote. This means that fast-diffusing MEX-5 and PIE-1 proteins are approximately symmetrically distributed, whereas the corresponding slow-diffusing proteins are highly enriched in the anterior and posterior cytoplasm, respectively. We have also applied our mathematical theory of space-dependent switching diffusivities to derive explicit formulae for intracellular concentration gradients in *C. elegans* [4], which closely match the experimental and numerical results of [14].

In this paper, we further extend the theory of space-dependent switching diffusivities by considering the effects of cellular microstructures. We can think of this microstructure as reflecting localized cellular substrates that a diffusing particle can temporarily bind to, thereby entering a slower diffusive state. Suppose that a particle can switch between two states $n = 0, 1$ with diffusivities D_n according to a two-state Markov process

$$D_0 \underset{\alpha_1/\epsilon}{\overset{\alpha_0/\epsilon}{\rightleftharpoons}} D_1,$$

where $\alpha_{0,1} = O(1)$ and ϵ is a scale factor. Furthermore, we assume that the switching rate out of state n depends on a macrostructure determined by $x \in \Omega \subset \mathbb{R}^d$, and a microstructure determined by x/δ, where $0 < \delta \ll 1$ is the scale of the microstructure in the cell. That is, $\alpha_n = \alpha_n(x, x/\delta)$. An example is shown in Figure 1, where α_0 is constant, whereas α_1 has a monotonically increasing macrostructure superimposed on a fast, spatially oscillating microstructure. We will use a combination of asymptotic analysis and the method of multiple scales to investigate the fast switching limit $\epsilon \to 0$ and the homogenization limit $\delta \to 0$. In particular, we will demonstrate that the averaged system obtained by taking both limits depends on which order they are taken.

2. Switching diffusivities with spatial microstructure. Let $u_n(x,t)$ denote the concentration of proteins diffusing with diffusivity D_n, $n = 0, 1$, in a bounded region $\Omega \subset \mathbb{R}^d$. The switching rates are given by $\frac{1}{\epsilon}\alpha_n\left(x, \frac{x}{\delta}\right)$, with $0 < \epsilon \ll 1$ designating the timescale of the switching and δ determining the spatial scale of the cellular microstructure. We further assume that the switching rates are bounded at the microscale

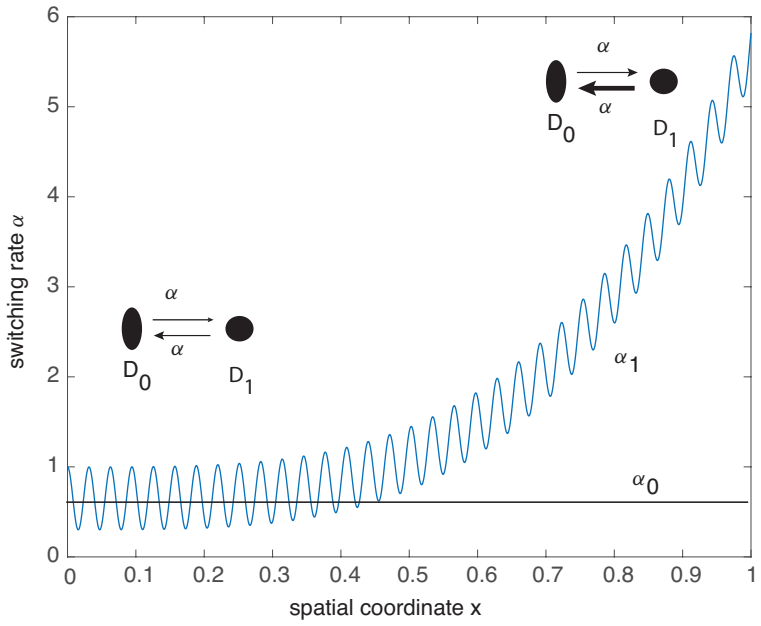

FIG. 1. *Schematic illustration of a spatially varying switching rate with both macrostructure and microstructure. A Brownian particle randomly switches between two conformational states $n = 0, 1$ having different diffusivities such that $D_0 < D_1$. The switching rate α_0 from state $n = 0$ is taken to be a constant. On the other hand, the switching rate α_1 from state $n = 1$ monotonically increases at the macroscale and periodically oscillates on the microscale. On average, the particle spends more time in the slow diffusing state at the end $x = 1$ and approximately the same time in both states at the end $x = 0$.*

$$0 < \alpha_{n,L}(x) \leq \alpha_n\left(x, \frac{x}{\delta}\right) \leq \alpha_{n,U}(x). \tag{2.1}$$

(These conditions help ensure that $\alpha_{0,1}$ both remain bounded at $O(1)$ throughout the domain and that the proportions $\alpha_{0,1}/\sum_n \alpha_n$ are always well defined.) To simplify the analysis, we take the switching rates to be periodic in the variable x/δ. The concentrations $u_0(x,t), u_1(x,t)$ then satisfy a system of the form

$$\frac{\partial u_n}{\partial t} = D_n \Delta u_n - \frac{1}{\epsilon}\alpha_n\left(x, \frac{x}{\delta}\right) u_n + \frac{1}{\epsilon}\alpha_{1-n}\left(x, \frac{x}{\delta}\right) u_{1-n} + f_n(x,t), \tag{2.2}$$

where $n = 0, 1$, $x \in \Omega \subset \mathbb{R}^d_+$ without loss of generality, and $f_n(x,t)$ is a function describing any sources or sinks for the protein concentration in state n within the domain. Note that we do not assign units to the space and timescales, but at the level of cellular processes, which we have in mind, the length scale is often measured in micrometers and the time scale in seconds. Throughout, we will use Neumann boundary conditions $\partial_\eta u_n\big|_{\partial\Omega} = 0$, where η represents the unit normal vector on the boundary of Ω.

Our main goal is to compare several system reductions. The first is a fast-switching limit $\epsilon \to 0$. In this limit, we can assume that a multitude of switching events occur while the position of a particle stays roughly the same. Define the probability that for fixed x a particle is in state n by

$$\rho_n\left(x, \frac{x}{\delta}\right) = \frac{\alpha_{1-n}\left(x, \frac{x}{\delta}\right)}{\alpha_n\left(x, \frac{x}{\delta}\right) + \alpha_{1-n}\left(x, \frac{x}{\delta}\right)}. \tag{2.3}$$

Let the total protein concentration be given by $u(x,t) = u_0(x,t) + u_1(x,t)$. The fast-switching reduction is then found by assuming

$$u_n = u\rho_n + \epsilon w_n \tag{2.4}$$

and substituting this into (2.2) to find an effective equation governing the total density $u(x,t)$.

On the other hand, the presence of a microstructure suggests that there are effective switching rates $\alpha_n^e(x)$ given by homogenizing in some proper way. These rates can be found by utilizing the method of multiple scales. Assume the micro- and macroscales are independent by setting $y = x/\delta$. We assume that the microstructure variable y is in $\mathbb{R}^d$. Since we restricted $\alpha_n(x,y)$ to be periodic in y, there exists a vector y_p such that

$$\alpha_n(x, y + y_p) = \alpha_n(x,y) \quad \text{for all } x, y.$$

We can then restrict the y domain to a bounded region $\Omega_y \subset \mathbb{R}^d$ defined by $\Omega_y = [0, y_{p,1}] \times \cdots \times [0, y_{p,d}]$ and then extend any solution to the rest of the domain using periodicity.

Under the separation of scales, the differential operator then becomes $\nabla \to \nabla_x + \frac{1}{\delta}\nabla_y$. Expanding u_n in powers of δ

$$u_n(x,t) = u_n^{(0)}(x,y,t) + \delta u_n^{(1)}(x,y,t) + \delta^2 u_n^{(2)}(x,y,t) + O(\delta^3), \tag{2.5}$$

and again substituting into (2.2) results in a hierarchy of equations at different orders. Enforcing solvability conditions allows us to derive effective equations for $u_n(x,t)$. This is a classical approach, an extensive general theory of which can be found in [11].

Performing both of these procedures allows us to find effective equations and solutions in the limits $\epsilon \to 0$ and $\delta \to 0$, but it is unclear in which order to take these limits. We will show that there are qualitative and quantitative differences between the two cases and illustrate these differences with some examples.

2.1. Limit order $\epsilon \to 0$ then $\delta \to 0$. We first perform the fast-switching reduction. Substituting $u_n = \rho_n u + \epsilon w_n$ into (2.2), summing over n, and requiring that $w_0 + w_1 = 0$ yields the equation

$$\frac{\partial u}{\partial t} = \Delta\left(\overline{D}\left(x, \frac{x}{\delta}\right) u\right) + f(x,t), \quad \partial_\eta[\overline{D}u]\big|_{\partial\Omega} = 0, \tag{2.6}$$

where we have defined an effective diffusion coefficient $\overline{D}$ by

$$\overline{D}\left(x, \frac{x}{\delta}\right) = D_0\rho_0\left(x, \frac{x}{\delta}\right) + D_1\rho_1\left(x, \frac{x}{\delta}\right), \tag{2.7}$$

and let $f(x,t) = \sum_n f_n(x,t)$.

We now homogenize by setting $y = x/\delta$, $\nabla \to \nabla_x + \frac{1}{\delta}\nabla_y$ and expanding

$$u(x,t) = u^{(0)}(x,y,t) + \delta u^{(1)}(x,y,t) + \delta^2 u^{(2)}(x,y,t) + O(\delta^3). \tag{2.8}$$

The $O(1/\delta^2)$ equation is

$$\Delta_y\left[\overline{D}(x,y)u^{(0)}\right] = 0. \tag{2.9}$$

We require that the solution is periodic and bounded in the microstructure variable y. By Liouville's theorem, the only periodic bounded solutions are constant in y, hence

$$\overline{D}(x,y)u^{(0)}(x,y,t) = c_0(x,t). \tag{2.10}$$

At $O(1/\delta)$ we have

$$\Delta_y \left[\overline{D}(x,y)u^{(1)}\right] + 2\nabla_x \cdot \nabla_y \left[\overline{D}(x,y)u^{(0)}\right] = 0. \tag{2.11}$$

Since $\overline{D}(x,y)u^{(0)} = c_0(x,t)$ is independent of y, the solution is again of the form

$$\overline{D}(x,y)u^{(1)}(x,y,t) = c_1(x,t). \tag{2.12}$$

Finally, the $O(1)$ equation is

$$\Delta_y \left[\overline{D}(x,y)u^{(2)}\right] + 2\nabla_x \cdot \nabla_y \left[\overline{D}(x,y)u^{(1)}\right] + \Delta_x \left[\overline{D}(x,y)u^{(0)}\right] = \frac{\partial u^{(0)}}{\partial t} - f(x,t). \tag{2.13}$$

Again, since $\overline{D}(x,y)u^{(1)} = c_1(x,t)$ does not depend on y, this reduces to

$$\Delta_y \left[\overline{D}(x,y)u^{(2)}\right] = \frac{\partial u^{(0)}}{\partial t} - \Delta_x \left[\overline{D}(x,y)u^{(0)}\right] - f(x,t). \tag{2.14}$$

Note that the adjoint operator to $\Delta_y \overline{D}(x,y)$ is $\overline{D}(x,y)\Delta_y$, whose null space includes constants in y. By the Fredholm alternative, to have a solution for $\overline{D}(x,y)u^{(2)}$ we must therefore have

$$\int_{\Omega_y} \frac{\partial u^{(0)}}{\partial t} - \Delta_x \left[\overline{D}(x,y)u^{(0)}\right] - f(x,t)\, dy = 0, \tag{2.15}$$

where the integration is done with respect to the microscale y. Therefore, since $\overline{D}(x,y)u^{(0)} = c_0(x,t)$, we must have

$$\langle \overline{D}^{-1} \rangle_\infty \frac{\partial \left[\, \overline{D}(x,y)u^{(0)}\right]}{\partial t} - \Delta_x \left[\overline{D}(x,y)u^{(0)}\right] - f(x,t) = 0, \tag{2.16}$$

where

$$\langle \overline{D}^{-1} \rangle_\infty = \langle \overline{D}^{-1} \rangle_\infty(x) = \frac{1}{|\Omega_y|} \int_{\Omega_y} \overline{D}(x,y)^{-1}\, dy \tag{2.17}$$

is the harmonic mean of the effective diffusion coefficient with respect to the microstructure variable y. Note that $|\Omega_y|$ can be computed simply by using $|\Omega_y| = \prod_{k=1}^{d} |y_{p,k}|$. In one dimension, this reduces to

$$\langle \overline{D}^{-1} \rangle_\infty(x) = \frac{1}{y_p} \int_0^{y_p} \overline{D}(x,s)^{-1} ds. \tag{2.18}$$

In (2.16), the Laplacian Δ with respect to both scales has been replaced with the Laplacian Δ_x with respect to only the macroscale. Finally, if (2.16) holds, then the Fredholm alternative is satisfied for any function in the nullspace of the adjoint operator, completing the argument.

In the case $f(x,t)=0$, we have a steady-state solution to (2.16) given by

$$u^{(0)}(x,y)=\frac{A}{\overline{D}(x,y)}. \tag{2.19}$$

At this point we can average out the microstructure by integrating the solution over the cell Ω_y. This yields

$$u^{(0)}(x)=A\langle \overline{D}^{-1}\rangle_\infty(x). \tag{2.20}$$

Lastly, A can be determined by the normalization condition

$$A=u^*\left[\int_\Omega \langle \overline{D}^{-1}\rangle_\infty(x)\,dx\right]^{-1}, \tag{2.21}$$

where u^* is the total concentration in the domain Ω, which is conserved due to the no-flux boundary conditions.

There are a few things here to note. The first is that this reduction process introduces a boundary layer of order $\sqrt{\epsilon}$ around $\partial\Omega$ due to changes in the boundary conditions when taking the fast-switching limit. Higher order correction terms can be introduced if needed, as was done for $d=1$ in [4]. Second, for this order of limits, we did not need to assume that the switching rates were periodic in the microstructure if we are only interested in the steady-state problem $\frac{\partial u^{(0)}}{\partial t}=0$. Alternatively, we could work with nonperiodic α_0 and α_1 by defining $\Omega_r=\{y\in\mathbb{R}^d_+ : \|y\|<r\}$, and setting

$$u^{(0)}(x)=\lim_{r\to\infty}\frac{1}{|\Omega_r|}\int_{\Omega_r}u(x,y)\,dy, \tag{2.22}$$

which would instead yield

$$u^{(0)}(x)=A\langle \overline{D}^{-1}\rangle_\infty(x), \tag{2.23}$$

where

$$\langle \overline{D}^{-1}\rangle_\infty(x)=\lim_{r\to\infty}\frac{1}{|\Omega_r|}\int_{\Omega_r}\overline{D}(x,y)^{-1}\,dy. \tag{2.24}$$

In one dimension, this would reduce to

$$\langle \overline{D}^{-1}\rangle_\infty(x)=\lim_{y\to\infty}\frac{1}{y}\int_0^y \overline{D}(x,s)^{-1}ds. \tag{2.25}$$

The arguments with the Fredholm alternative would also still carry through. Since the nullspace of the adjoint operator would still contain constants in y, and the right hand side of (2.14) is independent of y, the argument still holds.

2.2. Limit order $\delta\to 0$ then $\epsilon\to 0$. Now we will instead first homogenize the system of equations using the method of multiple scales by setting $y=x/\delta$ and expanding
At $O(1/\delta)$ we have

$$u_n(x,t)=u_n^{(0)}(x,y,t)+\delta u_n^{(1)}(x,y,t)+\delta^2u_n^{(2)}(x,y,t)+O(\delta^3). \tag{2.26}$$

The $O(1/\delta^2)$ equation is

$$D_n\Delta_y u_n^{(0)}=0. \tag{2.27}$$

Again by Louville's theorem, the only bounded solutions are constant in y, therefore

$$u_n^{(0)}(x,y,t) = u_n^{(0)}(x,t). \tag{2.28}$$

$$D_n \Delta_y u_n^{(1)} + 2D_n \nabla_x \cdot \nabla_y u_n^{(0)} = 0. \tag{2.29}$$

Similar to before, we have that the second term vanishes since $u_n^{(0)}$ does not depend on y, therefore

$$u_n^{(1)}(x,y,t) = u_n^{(1)}(x,t). \tag{2.30}$$

Finally, the $O(1)$ equation is

$$\begin{aligned} D_n \Delta_y u_n^{(2)} + 2D_n \nabla_x \cdot \nabla_y u_n^{(1)} &= -D_n \Delta_x u_n^{(0)} \\ &+ \frac{\partial u_n^{(0)}}{\partial t} + \frac{1}{\epsilon}\alpha_n(x,y)u_n^{(0)} - \frac{1}{\epsilon}\alpha_{1-n}(x,y)u_{1-n}^{(0)} - f_n(x,t). \end{aligned} \tag{2.31}$$

Similar to before, the term involving $u_n^{(1)}$ vanishes. Notice that unlike when we took the fast-switching limit first, the right-hand side at $O(1)$ is now dependent on the microstructure variable y.

Since the only periodic bounded functions that are solutions to $\Delta_y u_n = 0$ are constants, the Fredholm alternative gives us that the right-hand side of (2.31) must satisfy

$$\frac{1}{|\Omega_y|}\int_{\Omega_y} -D_n \Delta_x u_n^{(0)} + \frac{\partial u_n^{(0)}}{\partial t} + \frac{1}{\epsilon}\alpha_n(x,y)u_n^{(0)} - \frac{1}{\epsilon}\alpha_{1-n}(x,y)u_{1-n}^{(0)} - f_n(x,t)\,dy = 0. \tag{2.32}$$

Since only α_0 and α_1 depend on y, (2.32) reduces to

$$\frac{\partial u_n^{(0)}}{\partial t} = D_n \Delta_x u_n^{(0)} - \frac{1}{\epsilon}\alpha_n^e(x)u_n^{(0)} + \frac{1}{\epsilon}\alpha_{1-n}^e(x)u_{1-n}^{(0)} + f_n(x,t), \tag{2.33}$$

where we have defined the effective switching rate over a period α_n^e by

$$\alpha_n^e(x) = \frac{1}{|\Omega_y|}\int_{\Omega_y} \alpha_n(x,y)\,dy. \tag{2.34}$$

We can now take a fast switching limit $\epsilon \to 0$ like before, setting $u_n^{(0)} = u^{(0)}\rho_n^e + \epsilon w_n$ where now

$$\rho_n^e(x) = \frac{\alpha_{1-n}^e(x)}{\alpha_0^e(x) + \alpha_1^e(x)}. \tag{2.35}$$

The procedure is now the same as before, so we will just summarize the result below. Summing (2.33) over n yields

$$\Delta_x\left[\overline{D}_e(x)u^{(0)}\right] = 0, \tag{2.36}$$

with boundary conditions

$$\partial_\eta \left[\overline{D}_e u^{(0)} \right] |_{\partial\Omega} = 0, \tag{2.37}$$

where the effective diffusion coefficient is defined by

$$\overline{D}_e(x) = D_0 \rho_0^e(x) + D_1 \rho_1^e(x). \tag{2.38}$$

Solving explicitly for the protein concentration, we find that

$$u^{(0)}(x) = \frac{A}{\overline{D}_e(x)} \tag{2.39}$$

with normalization constant

$$A = u^* \left[\int_\Omega \overline{D}_e^{-1}(x) dx \right]^{-1}. \tag{2.40}$$

3. Examples in $d = 1$ space dimension. We now have two different approximate solutions based on taking the limits $\epsilon \to 0$ and $\delta \to 0$ in different orders. The question naturally arises whether or not the order of limits differs significantly. We will show that they do by considering a number of examples of space-dependent switching rates in one dimension. We also take $f_n = 0$, $D_0 = 0.1$, $D_1 = 5$, and normalize all solutions so that the total concentration is unity.

As our first example, let $\Omega = (0, \pi)$ and

$$\alpha_n(x, x/\delta) = x^4 \sin^2(x/\delta + \phi_n) + 1, \tag{3.1}$$

so that $y_p = \pi$. The switching rates are then identical, save for a phase shift ϕ_n in the microstructure. This can be thought of as corresponding to localized regions where a single particle is much more likely to bind to another particle, entering a slow diffusive state, and regions where the reverse holds instead. The degree of separation between these regions is captured by $\phi_0 - \phi_1$. We take $\phi_0 = 0$, $\phi_1 = \phi$. The key here is that if we homogenize first (meaning, take $\delta \to 0$ first), we end up with

$$\alpha_0^e(x) = \alpha_1^e(x) = \frac{x^4}{2} + 1 \tag{3.2}$$

since the average value of a periodic function over one period does not depend on the phase shift ϕ. This means that if we perform the limits in the order $\delta \to 0$, then $\epsilon \to 0$, we will end up with an effective diffusion coefficient given by $\overline{D} = D_0/2 + D_1/2$, indicating that the solution to the reduced equation is simply

$$u^{(0)}(x) = \frac{1}{\pi}. \tag{3.3}$$

However, if we take limits in the reverse order, we end up with an effective averaged solution

$$u^{(0)}(x) = A \langle \overline{D}^{-1} \rangle_\infty(x) \tag{3.4}$$

with

$$\langle \overline{D}^{-1} \rangle_\infty(x) = \frac{1}{y_p} \int_0^{y_p} \overline{D}(x, y)^{-1} dy \tag{3.5}$$

and

$$A = u^* \left[\int_0^\pi \langle \overline{D}^{-1} \rangle_\infty (x) dx \right]^{-1}. \tag{3.6}$$

Since we are no longer averaging the switching rates individually, and instead averaging the reciprocal of the effective diffusion coefficient, we no longer have a constant solution unless $\phi = 0$. In the case of maximal separation $\phi = \pi/2$, the difference in the order of limits is most apparent, as illustrated in Figure 2.

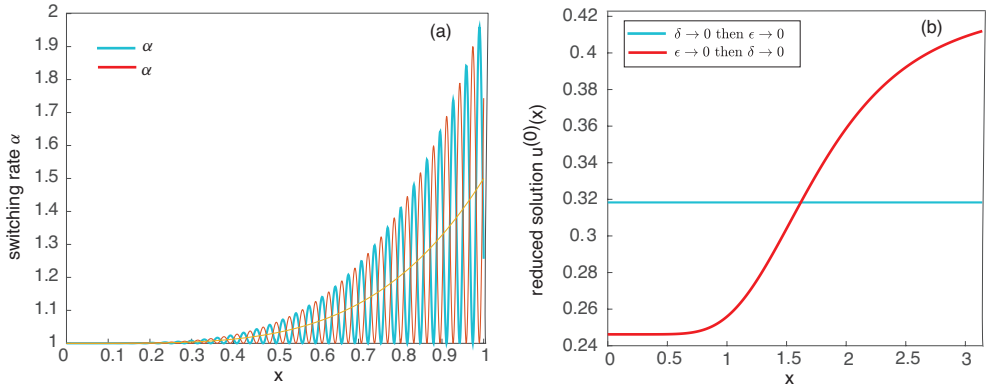

FIG. 2. *Spatially varying switching rates given by* (3.1) *with* $\phi_0 = 0$ *and* $\phi_1 = \pi/2$. (a) *Plot of switching rates as a function of* x. *Both have the same spatially averaged switching rate (indicated by the monotonically increasing curve).* (b) *Plot of leading-order averaged concentration* $u^{(0)}(x)$ *as a function* x *for the two limit orders. Note that the solutions are normalized so that the total concentration is unity.*

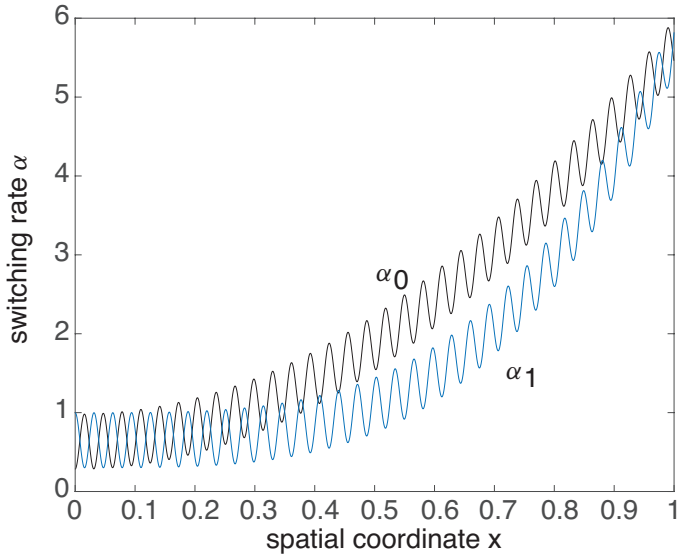

FIG. 3. *Spatially varying switching rates given by* (3.7) *with* $\delta = 0.02$.

In the above example, we assumed that the two switching rates had the same macrostructure, which was modulated by the microstructure. Let us now consider an example where both the macro- and microstructures differ (see Figure 3):

(3.7)
$$\alpha_0(x, x/\delta) = 5x^2 + 0.7\sin^2(x/\delta) + 0.3, \quad \alpha_1(x, x/\delta) = 5x^{3.5} + 0.7\sin^2(x/\delta + \pi/2) + 0.3.$$

In contrast to the previous example, the microstructure is now an additive rather than a multiplicative term. Consequently, it is only significant for small values of x. Again we find that in this regime, the reduction of the full solution depends on the order with which the limits are taken; see Figure 4. Interestingly, both limit orders follow the general trend of the full solution. However, we find that it is more appropriate to take the fast switching limit first when $\epsilon \ll \delta$, while homogenization as a first step is a better approximation when $\delta \ll \epsilon$. This also holds for larger x, as can be seen in Figure 5 by zooming in on the plots. Based on our numerical studies, it appears that a crossover regime $\epsilon = \delta^2$ seems to be the dividing case where neither approximation works much better than the other. This is likely related to the fact that this is the diffusive scaling of the diffusion equation.

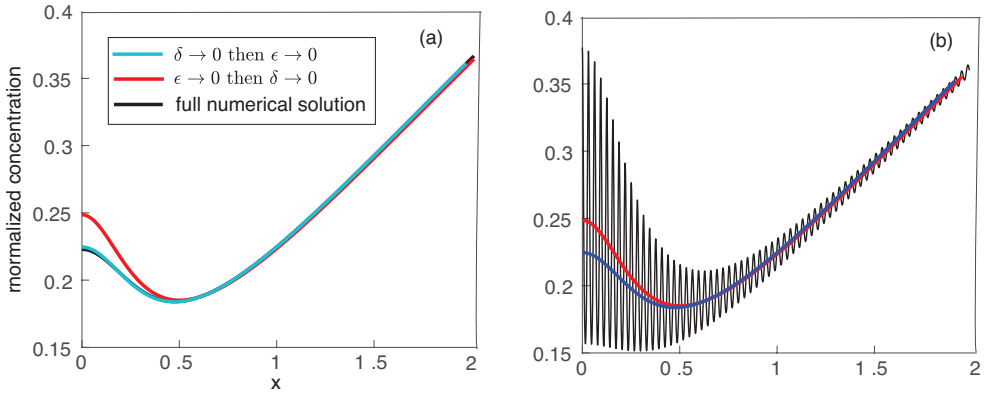

FIG. 4. *Spatially varying switching rates given by* (3.7). *Comparison between full solution and the two different order limits for* (a) $\epsilon = 10^{-2}$, $\delta = 10^{-3}$ *and* (b) $\epsilon = 10^{-5}$, $\delta = 10^{-2}$. *In* (a), *homogenizing the spatial structure prior to the fast-switching limit provides a better approximation, while the opposite is true in* (b) *(see magnified figures below).*

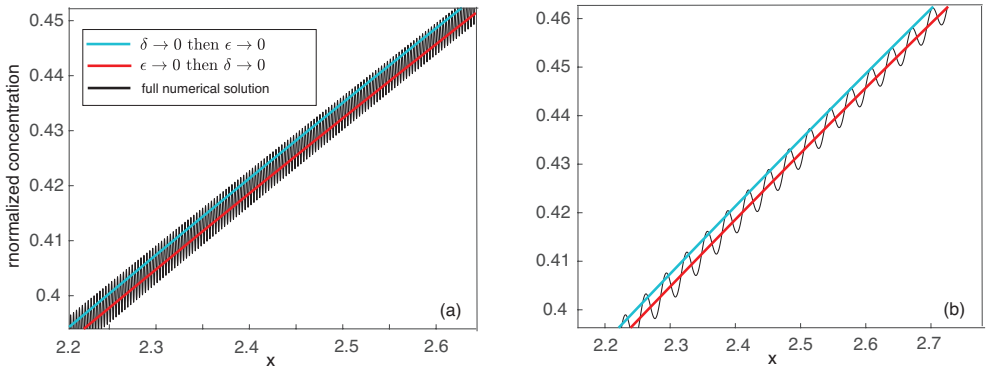

FIG. 5. *Magnified verison of Figure* 4 *for* (a) $\epsilon = 10^{-6}$, $\delta = 10^{-3}$ *and* (b) $\epsilon = 10^{-5}$, $\delta = 10^{-2}$.

To see one connection with the diffusive scaling, we consider a simplified version of our original equation (2.2), taking no macrostructure dependence in the switching rates and setting $f_n(x,t) = 0$:

$$\frac{\partial u_n}{\partial t} = D_n \Delta u_n - \frac{1}{\epsilon}\alpha_n(x/\delta)u_n + \frac{1}{\epsilon}\alpha_{1-n}(x/\delta)u_{1-n}. \tag{3.8}$$

Assuming that we are in the regime $\epsilon = \delta^2$, we can introduce the scaling $x/\delta \to x$, $t/\delta^2 \to t$ to arrive at

$$\frac{\partial u_n}{\partial t} = D_n \Delta u_n - \alpha_n(x)u_n + \alpha_{1-n}(x)u_{1-n}. \tag{3.9}$$

The resulting reaction-diffusion equation does not depend on either small parameter, and under our assumptions it is intractable to small-parameter approximations. This suggests that any asymptotic analysis would need to be done prior to rescaling.

Since the analysis in previous sections does not cover this borderline case $\epsilon = \delta^2$, an asymptotic approximation with respect to only a single small parameter δ would need to be developed. While this is fairly straightforward if there is no explicit dependence on the macrostructure, this particular case for the switching rates results in an approximate steady-state that is constant throughout the domain, just as in sections 2.1 and 2.2. Extending an asymptotic analysis to the case of an explicit macrostructure in the switching rates is a harder problem that we leave open.

4. Mean First Passage Time Analysis. The steady-state analysis and asymptotics in the previous sections provide insights into the global effects of the presence of a cellular microstructure, particularly in cases where there are highly local regions with a higher or lower chance of affecting the diffusivity of a diffusing protein. However, the average effect of this microstructure from the perspective of a single particle is unclear and remains of some interest. We will now seek to gain more information about such effects by investigating the mean first passage time (MFPT) for a particle starting at an initial location x to reach some portion of the boundary $\Gamma \subset \partial\Omega$. Intuitively, we expect that alternating regions of fast and slow switching will average out from the perspective of a traveling particle, and the MFPT should not exhibit a locally periodic structure, unlike the overall concentration profile.

We will first consider the MFPT problem for the full system. Let $X(t)$ be the location of a diffusing particle in Ω at time t. We want to calculate statistics for when this particle first reaches some subset $\Gamma \subset \partial\Omega$ of the boundary. Let

$$p_n(x,t) = p(x,t,n|z,0,m)$$

be the probability densities for the pair $(X(t), n(t))$ at time t conditioned on an initial location $X(0) = z$ and an initial diffusive state $m(t) = m$. Then $p_n(x,t)$ satisfies the same system of equations (2.2) as $u_n(x,t)$ with $f_n \equiv 0$ and the normalization condition

$$\int_\Omega \sum_n p_n(x,0)\,dx = 1. \tag{4.1}$$

Define a vector-valued function $\vec{p}(x,t)$ by

$$\vec{p}(x,t) = \begin{pmatrix} p_0(x,t) \\ p_1(x,t) \end{pmatrix}, \tag{4.2}$$

a transition matrix $A(x, x/\delta)$ by

$$A = \begin{pmatrix} \alpha_0 & -\alpha_1 \\ -\alpha_0 & \alpha_1 \end{pmatrix}, \tag{4.3}$$

and a diffusion tensor $\mathbf{D}$

$$\mathbf{D} = \begin{pmatrix} D_0 & 0 \\ 0 & D_1 \end{pmatrix}. \tag{4.4}$$

We can then write the forward Chapman–Kolmogorov (CK) equation for $\vec{p}$ as

$$\frac{\partial \vec{p}}{\partial t} = \mathbf{D}\Delta\vec{p} - \frac{1}{\epsilon}A\vec{p} \equiv \mathbb{L}\vec{p}. \tag{4.5}$$

Note that p_n specifies the diffusive state since the distinct diffusivities, $D_0 \neq D_1$, make finding a single equation for the total probability $p(x,t) = p_0(x,t) + p_1(x,t)$ nontrivial. Since we are interested in a first passage time (FPT) problem, we will impose a reflecting boundary condition $\partial_x \vec{p} = 0$ on $\partial\Omega \setminus \Gamma$ and an absorbing boundary condition $\vec{p} = 0$ on Γ.

Let T be the (stochastic) first time the particle reaches Γ. The FPT density conditioned on the initial diffusive state m of the particle is then defined by

$$f(z,t,m) = -\frac{\partial \mathbb{P}(z,t,m)}{\partial t}, \tag{4.6}$$

where the survival probability $\mathbb{P}$ is defined as

$$\mathbb{P}(z,t,m) = \int_\Omega \sum_n p(x,t,n|z,0,m)\, dx. \tag{4.7}$$

From $f(z,t,m)$, we can arrive at the MFPT $\tau(z,m)$ by

$$\tau(z,m) = \int_0^\infty t f(z,t,m) dt = \int_0^\infty \mathbb{P}(z,t,m) dt \tag{4.8}$$

after integrating by parts.

We can now derive an equation for τ by integrating the backward CK equation corresponding to (4.5) over $x \in \Omega$ then $t \in [0,\infty)$. The backward CK equation is

$$\frac{\partial \vec{q}}{\partial t} = \mathbb{L}^\dagger \vec{q}, \tag{4.9}$$

where now

$$\vec{q} := \sum_n \begin{pmatrix} p(x,t,n|z,0,0) \\ p(x,t,n|z,0,1) \end{pmatrix} =: \begin{pmatrix} q_0(x,t|z,0) \\ q_1(x,t|z,0) \end{pmatrix}, \tag{4.10}$$

and the subscript refers to the initial diffusive state m. Correspondingly, the Laplacian Δ in the adjoint operator $\mathbb{L}^\dagger = \mathbf{D}\Delta - \frac{1}{\epsilon}A^T$ is now applied to the initial position z. We will use the subscript m when referring to a quantity related to the initial diffusive state and reserve n for cases when the quantity corresponds to the forward CK equation. The boundary conditions in terms of z are still absorbing on Γ and reflecting on $\partial\Omega \setminus \Gamma$.

Now that we have the backward equation, integrating over space and time yields

$$\begin{pmatrix} -1 \\ -1 \end{pmatrix} = \mathbb{L}^\dagger \vec{\tau}, \tag{4.11}$$

with

$$\vec{\tau} = \begin{pmatrix} \tau(z,0) \\ \tau(z,1) \end{pmatrix} := \begin{pmatrix} \tau_0(z) \\ \tau_1(z) \end{pmatrix}. \tag{4.12}$$

To obtain an MFPT independent of the initial value of m, we define

$$\tau(z) = \sum_{m=0,1} \rho_m(z)\tau_m(z). \tag{4.13}$$

Here, $\rho_m(z)$ designates the probability that the particle is in state m, conditioned on the initial position $X(0) = z$. In the limit of fast switching $\epsilon \to 0$, we can assume that the particle switches states many times before moving a significant spatial distance, indicating that a particle instantaneously forgets its initial state in the limit $\epsilon \to 0$. Therefore, it is natural to take

$$\rho_m(z) = \frac{\alpha_{1-m}(z, z/\delta)}{\alpha_0(z, z/\delta) + \alpha_1(z, z/\delta)}. \tag{4.14}$$

Finally, since $\tau(z) = \mathbb{E}[T|X(0) = z]$, we can integrate τ over a distribution of initial locations $g(z)$ to obtain a space-independent MFPT that only depends on the geometry of the domain and the initial state of the diffusing particle

$$\overline{\tau} = \int_\Omega \tau(z)g(z)\,dz = \int_\Omega \left(\sum_{m=0,1} \tau_m(z)\rho_m(z) \right) g(z)\,dz. \tag{4.15}$$

Several natural choices for $g(z)$ are a uniform distribution $g(z) = 1/|\Omega|$, a distribution based on the initial concentration profile $g(z) = u(x,0)/\|u(x,0)\|$, and a distribution based on the steady-state concentration profile $g(z) = u(x,\infty)/\|u(x,\infty)\|$.

Investigating numerical solutions for the MFPT problem, we find that the microstructure does not directly appear in $\tau(z)$. This is a reasonable result since for a FPT statistic, intuition would suggest alternating regions of high and low diffusivity will average out as a single particle diffuses between them, especially if the variation is at a much finer scale than any macrostructure effects. To make this precise, one can look at fast switching and homogenization reductions with regard to the MFPT equation. We will not go through the details, but it is straightforward to show that in the limits $\epsilon \to 0$ then $\delta \to 0$, the resulting MFPT problem to leading order takes the form of Poisson's equation

$$\Delta_z \tau^{(0)}(z) = -\langle \overline{D}^{-1} \rangle_\infty(z), \tag{4.16}$$

where the effective diffusion coefficient is as previously defined and with boundary conditions

$$\partial_\eta \tau^{(0)}(z)\big|_{\partial\Omega\setminus\Gamma} = 0,\ \tau^{(0)}(z)\big|_\Gamma = 0. \tag{4.17}$$

For the limits $\epsilon \to 0$ then $\delta \to 0$, the resulting MFPT problem to leading order has a similar form

$$\Delta \tau^{(0)} = \frac{-1}{\overline{D}_e(z)}, \tag{4.18}$$

$$\partial_\eta \tau^{(0)}(z)\big|_{\partial\Omega\setminus\Gamma} = 0,\ \tau^{(0)}(z)\big|_\Gamma = 0, \tag{4.19}$$

with

$$\overline{D}_e(z) = D_0 \frac{\alpha_1^e(z)}{\alpha_0^e(z)+\alpha_1^e(z)} + D_1 \frac{\alpha_0^e(z)}{\alpha_0^e(z)+\alpha_1^e(z)}, \tag{4.20}$$

where we have now averaged the switching rates prior to defining the effective diffusion coefficient. In one dimension with $\Omega = (0, L)$ and $\Gamma = \{0, L\}$, these two equations have respective explicit solutions

$$\tau^{(0)}(z) = \int_0^L \int_0^{z'} \langle \overline{D}^{-1} \rangle_\infty (z') dz'' dz' - \int_0^z \int_0^{z'} \langle \overline{D}^{-1} \rangle_\infty (z'') dz'' dz' \tag{4.21}$$

and

$$\tau^{(0)}(z) = \int_0^L \int_0^{z'} \frac{1}{\overline{D}_e(z)} dz'' dz' - \int_0^z \int_0^{z'} \frac{1}{\overline{D}_e(z)} dz'' dz'. \tag{4.22}$$

Using another example of switching rates (see Figure 6), we compare the two types of limits to the original numerical solution of the MFPT. The results are shown in Figure 7. It is worth observing that the same separation regime for ϵ and δ is apparent here, with $\epsilon \to 0$ first a better match when $\epsilon \ll \delta^2$, $\delta \to 0$ first a better fit when $\epsilon \gg \delta^2$, and $\epsilon = \delta^2$ a regime where neither asymptotic solution seems to do better, although they again still follow the trend of the full problem. Another point of interest is that in all the cases that we tested, the two asymptotic solutions were upper and lower bounds for the true MFPT. In particular, taking $\delta \to 0$ first provides a lower bound, while $\epsilon \to 0$ first yields an upper bound.

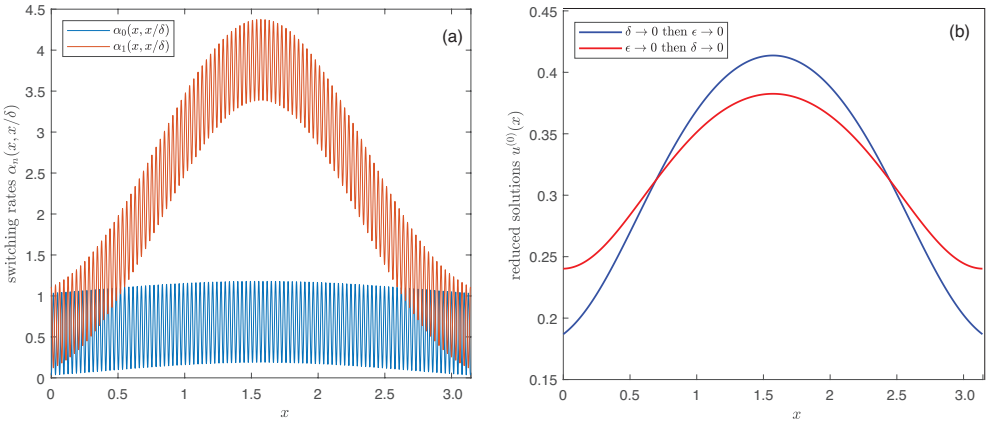

FIG. 6. (a) *Another example of spatially varying switching rates:* $\alpha_0(x, x/\delta) = 0.01(x+0.5)^2(x-L-0.5)^2 + \sin^2(x/\delta)$ *and* $\alpha_1(x, x/\delta) = 0.01(x+0.5)^4(x-L-0.5)^4 + \sin^2(x/\delta+\pi/2)$. (b) *Plot of leading-order averaged concentration* $u^{(0)}(x)$ *as a function* x *for the two limit orders.*

So far, we have formulated the FPT problem for the full system and then investigated the limits $\epsilon, \delta \to 0$. A natural question is whether or not one obtains the same results if one takes the joint limits first and then derives the MFPT starting from the averaged system. It is straightforward but tedious to show that for the limits $\lim_{\epsilon\to 0}$, $\lim_{\delta\to 0}$, and $\lim_{\epsilon\to 0}\lim_{\delta\to 0}$, it does not matter when the MFPT problem is formulated. Simply put, deriving the MFPT before, in between, or after taking any of the above limits does not change the resulting derivation. The only key observation

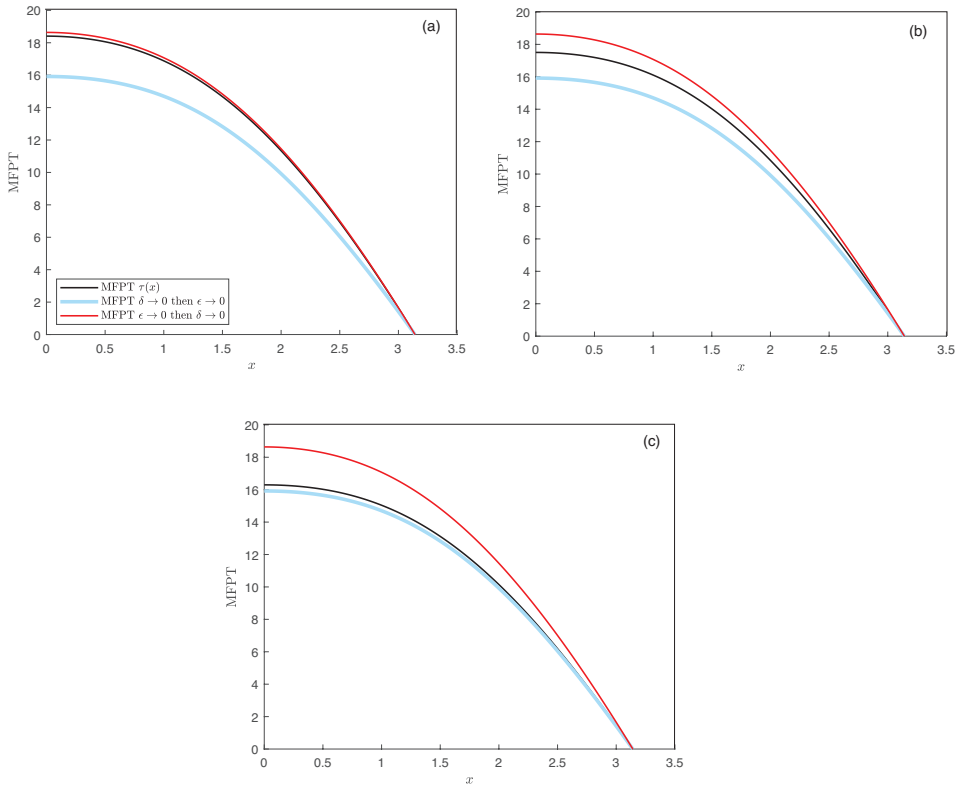

FIG. 7. *Mean first passage time $\tau(z)$ as a function of initial position z for* (a) $\epsilon = 10^{-5}$, (b) $\epsilon = 10^{-4}$, *and* (c) $\epsilon = 10^{-3}$. *The switching rates are as in Figure* 6. *Note that the microstructure appears to already be averaged out for this particular statistic of the system.*

needed for these cases is that in the limit $\epsilon \to 0$, the initial probability distribution $\rho_n^*(z)$ that a particle starting at z is initially in state n converges to the probability distribution $\rho_n(z)$. That is, the initial state is forgotten infinitely quickly in the fast-switching limit. The troublesome case seems to be $\lim_{\delta\to 0}\lim_{\epsilon\to 0}$. This is a result of the fast switching limit $\epsilon \to 0$ changing the structure of the differential operator. In particular, this limit introduces an effective diffusion operator of Itô form $\Delta\overline{D}(x, x/\delta)$ that captures the effects of the microstructure in place of the switching rates. The effective diffusion coefficient $\overline{D}(x, x/\delta)$ is the only place in the resulting system of PDEs where the microscale variable $y = x/\delta$ appears and creates issues when considering whether to homogenize prior to formulating the MFPT.

To highlight the issue, we will attempt to find an MPFT equation after applying both limits. We first consider (2.16) with a probabilistic formulation $u_n = p_n$, $f_n = 0$ and reflecting and absorbing boundary conditions as before. The resulting equation after applying limits is

$$\langle \overline{D}^{-1} \rangle_\infty \frac{\partial \left[\overline{D}(x,y) p^{(0)} \right]}{\partial t} = \Delta_x \left[\overline{D}(x,y) p^{(0)} \right]. \tag{4.23}$$

Where the product $c_0 = \overline{D}p^{(0)}$ is independent of the variable y. We can immediately see a complication as the homogenization in section 2 actually eliminated the microstructure for $c_0(x,t) = \overline{D}(x,y)p^{(0)}(x,y)$ due to the change in the structure of

the operator, so (2.16) is actually an equation for c_0 in terms of independent variables x and t. This is undesirable since we want an equation for the probability $p^{(0)}$ independent of y to derive the backward CK equation. If we rewrite (2.16) in terms of $p^{(0)}$, we end up with

$$\frac{\partial p^{(0)}}{\partial t} = \frac{1}{\langle \overline{D}^{-1} \rangle_\infty(x) \overline{D}(x,y)} \Delta_x \left[\overline{D}(x,y) p^{(0)} \right], \tag{4.24}$$

from which it is uncertain how to go about formulating the MFPT, as it is not clear if the survival probability $\mathbb{P}$ would satisfy the adjoint equation to (4.24).

5. Discussion. We investigated a cellular reaction-diffusion system inspired by recent results in cell polarization. This model incorporates both fast switching based on a small parameter ϵ and a local microstructure whose scale is determined by a second small parameter δ. The two small parameter limits $\delta \to 0$ (homogenization limit) and $\epsilon \to 0$ (fast switching limit) do not commute in general. The resulting reduced models approximate well the average of the full system in various parameter regimes. Based on numerical simulations, we find that the order of limits $\epsilon \to 0$, $\delta \to 0$ is a better approximation when $\epsilon \ll \delta^2$, while the order $\delta \to 0$, $\epsilon \to 0$ is more accurate if $\epsilon \gg \delta^2$; the separation seems to occur at the diffusive scaling $\epsilon = \delta^2$.

We also calculated statistics for an individual particle interacting with the cellular environment. In particular, we considered the MFPT for a diffusing protein to reach part of the cellular boundary given a starting location z, as this statistic can give a better sense of how the environment affects the transport of proteins. We found that the microstructure is averaged out when determining the MFPT, since a diffusing particle will tend to encounter many regions of faster or slower switching before reaching the boundary. One interesting observation is that taking $\epsilon \to 0$ then $\delta \to 0$ prior to formulating the MFPT problem is not the same as taking the respective limits after the formulation. The reaction-diffusion operator fundamentally changes form, seemingly preventing the classical formulation in the first place. The theoretical implications of this change in the form of the operator in the case of fast-switching and how this impacts the FPT problem is an interesting question that warrants further investigation.

REFERENCES

[1] P. C. Bressloff, *Stochastic switching in biology: from genotype to phenotype*, J. Phys. A: Math. Theoret., 50 (2017), 133001.

[2] P. C. Bressloff and S. D. Lawley, *Temporal disorder as a mechanism for spatially heterogeneous diffusion*, Phys. Rev. E, 95 (2017), 060101(R).

[3] P. C. Bressloff and S. D. Lawley, *Hybrid colored noise process with space-dependent switching rates*, Phys. Rev. E, 96 (2017), 012129.

[4] P. C. Bressloff, S. D. Lawley, and P. Murphy, *Protein concentration gradients and switching diffusions*, Phys. Rev. E, 99 (2019), 032409.

[5] R. Das, C. W. Cairo, and D. Coombs, *A hidden Markov model for single particle tracks quantifies dynamic interactions between LFA-1 and the actin cytoskeleton*, PLoS Comput. Biol., 5 (2009), e1000556.

[6] A. Godec and R. Metzler, *First passage time statistics for two-channel diffusion*, J. Phys. A, 50 (2017), 084001.

[7] P. C. Bressloff and S. D. Lawley, *Residence times of a Brownian particle with temporal heterogeneity*, J. Phys. A, 50 (2017), 195001.

[8] A. Kusumi, C. Nakada, K. Ritchie, K. Murase, K. Suzuki, H. Murakoshi et al., *Paradigm shift of the plasma membrane concept from the two-dimensional continuum fluid to the partitioned fluid: high-speed single-molecule tracking of membrane molecules*, Ann. Rev. Biophys. Biomol. Struct., 34 (2005), pp. 351–378.

[9] A. Kusumi, K. G. N. Suzuki, R. S. Kasai, K. Ritchieand, and T. K. Fujiwara, *Hierarchical mesoscale domain organization of the plasma membrane*, Trends Biochem. Sci., 36 (2011), pp. 604–615.

[10] F. Persson, M. linden, C. Unoson, and J. Elf, *Extracting intracellular diffusive states and transition rates from single-molecule tracking data*, Nat. Meth., 10 (2013), pp. 265–269.

[11] G. A. Pavliotis and A. M. Stuart, *Multiscale methods: averaging and homogenization*, 3rd. ed., Springer, New York, 2008.

[12] M. J. Saxton and K. Jacobson, *Single-particle tracking: applications to membrane dynamics*, Ann. Rev. Biophys. Biomol. Struct., 26 (1997), pp. 373–399.

[13] P. J. Slator, C. W. Cairo, and N. J. Burroughs, *Detection of diffusion heterogeneity in single particle tracking trajectories using a Hidden Markov Model with measurement noise propagation*, PLoS ONE, 10 (2015), e0140759.

[14] Y. Wu, B. Han, Y. Li, E. Munro, D. J. Odde, and E. E. Griffin, *Rapid diffusion-state switching underlies stable cytoplasmic gradients in the Caenorhabditis elegans zygote*, Proc. Natl. Acad. Sci., 115 (2018), pp. 8440–8449.

[15] E. Yamamoto, T. Akimotot, A. C. Kalli, K. Yasuoka, and M. S. P. Sansom, *Dynamic interactions between a membrane binding protein and lipids induce fluctuating diffusivity*, Sci. Adv., 3 (2017), e1601871.